

Original Articles

Remote sensing and optimized neural networks for landslide risk assessment: Paving the way for mitigating Afghanistan landslide damage

Ming Chang^{a,b,1}, Xiangyang Dou^{a,c,1}, Fenghuan Su^{b,*}, Bo Yu^a

^a State Key Laboratory of Geohazard Prevention and Geoenvironment Protection, Chengdu University of Technology, Chengdu 610059, Sichuan, China

^b Key Laboratory of Mountain Hazards and Earth Surface Processes, Chinese Academy of Sciences, Chengdu 610044, China

^c Faculty of Geo-Information Science and Earth Observation (ITC), University of Twente, 7522 NB, Enschede, Netherlands

ARTICLE INFO

Keywords:

Landslide
Afghanistan
Risk assessment
Remote sensing
Neural networks

ABSTRACT

Landslides caused by mega earthquakes and other extreme climate change pose a major threat to lives and infrastructure. However, the lack of a detailed and timely landslide inventory and relevant risk assessment attributable to ongoing conflicts limits the effective prevention measures in Afghanistan. This study presents the first landslide inventory covering the whole nation of Afghanistan from 2015 to the present utilizing Google Earth Pro imagery and manual interpretation. Based on this inventory of 3,260 mapped landslides, we analyzed the distributional characteristics of landslides in Afghanistan and conducted a risk assessment that included landslide susceptibility and hazard, and vulnerability of the bearing areas. The existing regional studies attest to the accuracy and reliability of the inventory, and the results of the risk assessment using the optimized neural network method in this study are well validated. This study can provide a good database for the Afghan government to carry out relevant pre-disaster warnings and post-disaster reconstruction, which can help to delineate hotspots where landslides may occur, and reduce potential economic losses and human casualties from future landslides.

1. Introduction

Landslides are among the most prevalent geological disasters worldwide (Causes, 2001; Huang and Fan, 2013), which pose a significant threat to both economic development and human safety. Co-seismic and post-seismic landslides following mega-earthquakes, whose activity may continue for up to a decade (Fan et al., 2019b). In 2022, a powerful earthquake of magnitude M_w 6.8 struck Luding County, China, triggering numerous coseismic landslides that destroyed homes, blocked roads, and caused many fatalities (Fan et al., 2022; Wang et al., 2022). Similarly, the M_w 7.9 Wenchuan earthquake of 2008 in China induced numerous landslides that resulted in significant human and economic losses (Chang et al., 2021; Fan et al., 2019a). In Taiwan, the 1999 Chi-Chi earthquake triggered over 20,000 landslides, while subsequent heavy rains in 2000 and 2001 caused even more landslides due to the high disturbance of surface strata (Lin et al., 2006). Consequently, researchers worldwide have undertaken investigations focusing on seismic activity, rainfall patterns, and other extreme weather-induced landslides, yielding preliminary findings. As almost all

earthquakes can lead to secondary disasters that may last for extended periods, conducting risk assessments is crucial for pre-disaster warning and post-disaster reconstruction efforts (Agung et al., 2023; Casagli et al., 2023; Chomba et al., 2022; Gariano and Guzzetti, 2016; Rosly et al., 2023).

A wide range of methods has been applied to assess the susceptibility of landslides, including logistic regression models (Dai et al., 2022), weight-of-evidence models (Chen et al., 2021), information quantity models (Tan et al., 2015), certainty factor methods (Yuan et al., 2022), fully connected neural network methods (Huang et al., 2020), neural network models (Gao and Ding, 2022), and others. Current researches proved that the selection of assessment models need comprehensively integrate local geological environments (Do et al., 2020; Shahabi et al., 2022; Zhang et al., 2022). The analytic hierarchy process is a widely used and scientifically proven multiple-criteria decision-making tool for geological hazard assessment, and is the preferred method for many scholars conducting susceptibility studies with good reliability and scientific validity (Kayastha et al., 2013; Vaidya and Kumar, 2006). Predominantly, vulnerability assessments of disaster-bearing bodies focus

* Corresponding author.

E-mail addresses: changmxq@126.com (M. Chang), douxyz1994@gmail.com (X. Dou), fhsu@imde.ac.cn (F. Su).

¹ These authors contributed equally to this work.

on factors including but not limited to population density, building density, land use, and major infrastructure projects (Glade, 2003; Van Westen et al., 2008). Following the Wenchuan earthquake, Chinese researchers have accrued substantial expertise in this domain, contributing to a more mature understanding of risk assessment in disaster-prone regions (Cui et al., 2012; Cui et al., 2009; Fan et al., 2018).

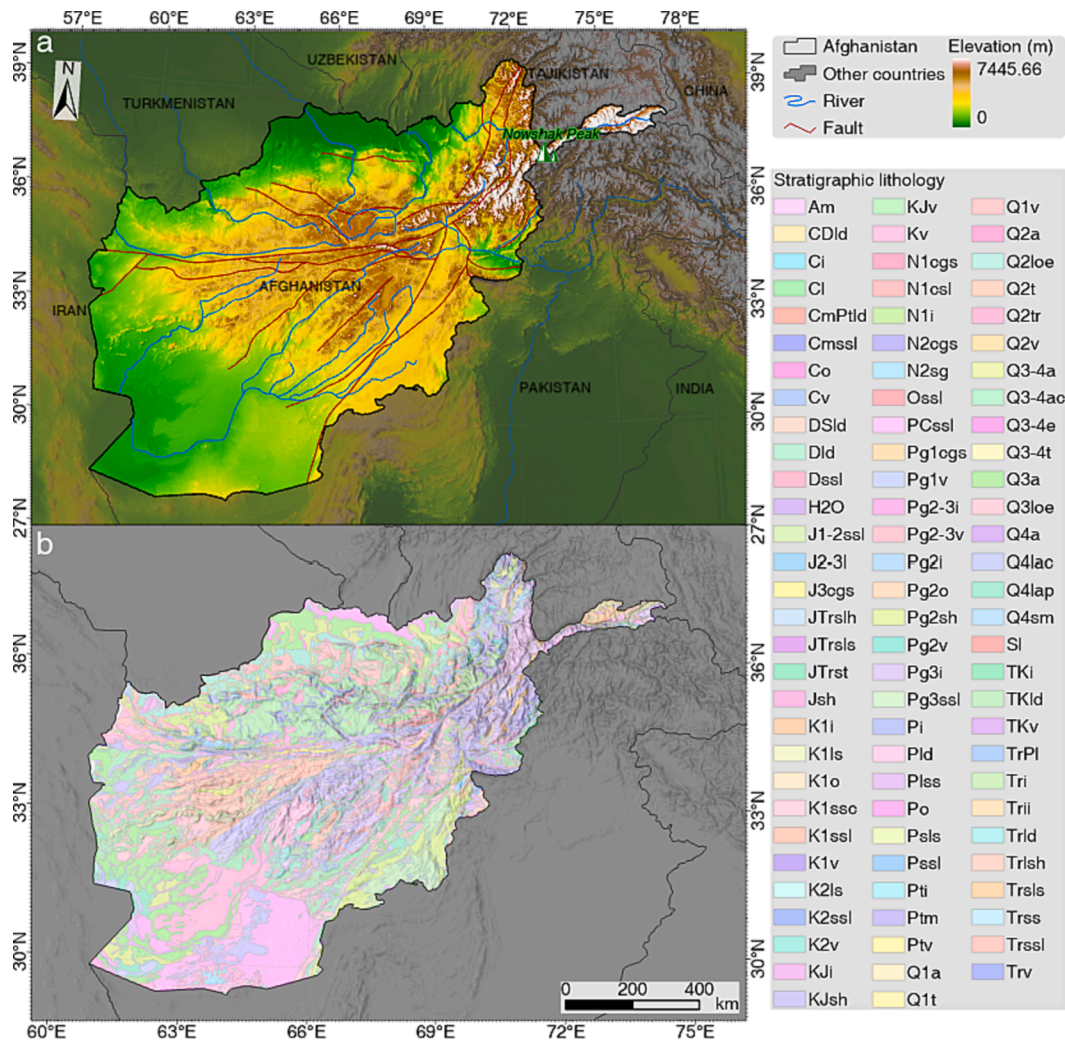
The persisting conflict in Afghanistan has notably impeded the comprehensive analysis and assessment of geohazards, primarily attributable to the country's economic instability and the humanitarian challenges it faces (Zhang et al., 2015). Nevertheless, several noteworthy studies have delved into the realm of geohazards within Afghanistan. Waseem et al. (2018), Boyd et al. (2007), and Menon et al. (2004) conducted separate assessments, focusing on historical earthquakes in the region. In parallel, Zhang et al. (2015) undertook a susceptibility assessment, specifically targeting the Abe Berek landslide in Badakhshan Province. Shroder et al. (2011b) made fairly strides by investigating and characterizing a total of 22 large geologic disasters, encompassing rockfalls, landslides, and debris flows in northeastern Afghanistan. Additionally, Shroder's work shed light on the occurrence of 34 large-scale loess landslides, often exacerbated by the frequency of earthquakes and agricultural land irrigation practices (Shroder et al., 2011a; Shroder et al., 2011b). Nonetheless, it is pertinent to note that these investigations primarily homed in on distinct regions or hydrological basins within Afghanistan's geographical confines. In light of the scarcity of prior research addressing the vulnerability of landslide-prone regions in Afghanistan and the challenges posed by on-site fieldwork,

our research endeavors to bridge this knowledge gap. Drawing upon established methodologies and insights gleaned from landslide vulnerability investigations in China, our study aspires to provide valuable insights into this hitherto underexplored domain.

Recognizing the importance of reducing the loss of life and property caused by landslides and ensuring the safety and efficacy of post-war reconstruction endeavors, a comprehensive quantitative risk assessment of landslides across Afghanistan is deemed a matter of notable research significance. To this end, we selected the entire nation of Afghanistan as our study area and meticulously interpreted all landslides that have occurred from 2015 to the present, utilizing Google Earth Pro (GEP) imagery. Our approach involved the utilization of the Analytic Hierarchy Process (AHP), the fully connected neural network (FCNN), and matrix analysis methods. These methods amalgamated geological conditions, earthquake magnitudes, precipitation data, and other predisposing factors with the vulnerability of populations exposed to disasters. By engaging in an exhaustive interpretation of landslides, our study culminated in a comprehensive landslide risk assessment for the entirety of Afghanistan. This study effectively fills a void in geohazard studies within Afghanistan and offers invaluable data support for humanitarian efforts in the region, carrying profound implications for guiding future endeavors in the country.

2. Study area

Afghanistan, a landlocked country in Central Asia, shares borders



with Turkmenistan, Uzbekistan, Tajikistan, China, Pakistan, and Iran (as shown in Fig. 1a) (Shahi, 2022). The Hindu Kush mountain range, located at the westernmost edge of the Tibetan Plateau (Dou et al., 2023), stretches across Afghanistan from northeast to southwest, giving rise to the remarkable Wakhan Corridor. With an area of approximately 647,500 km², Afghanistan is located on the Iranian plateau and is home to the Amu Darya, Kabul, Helmand, and Harirud rivers. Except for the southwest region, most of Afghanistan is comprised of alpine valleys, with 27% of the country's area at an elevation exceeding 2,500 m above sea level (a.s.l.), and its highest point, Nowshak Peak, reaching more than 7,400 m. Afghanistan's geological history is extensive, and it exhibits complete stratigraphic development from the oldest tertiary strata to the Holocene deposits (as shown in Fig. 1b) (Doeblich et al., 2006; Shroder et al., 2022). Numerous regions in Afghanistan are situated at high elevations, giving rise to low temperatures year-round and facilitating the formation of several glaciers and glacial lakes (Dou et al., 2023; Haritashya et al., 2009; Joya et al., 2021). Afghanistan is predominantly influenced by the subtropical high-pressure zone during the summer season, resulting in a dry climate with limited rainfall. The Indian Ocean is the primary source of moisture for the region. Annual rainfall in Afghanistan typically ranges around 350 mm and is mainly concentrated during the winter and spring seasons. Precipitation varies significantly with altitude and location, with a general pattern of decreasing from southeast to northwest. Alpine snow and glacial melt-water serve as crucial water sources for agricultural production (Aliyar and Esmailnejad, 2022; Roustae et al., 2020).

Due to Afghanistan's location as a landlocked country with high mountain growth and an active Alpine-Himalayan orogenic belt, it is highly susceptible to mega earthquakes (Waseem et al., 2018). These earthquakes can cause the mountains to crack, leading to geotechnical instability and an increased likelihood of landslides (Fan et al., 2019b). The current state of affairs in Afghanistan is marred by political turmoil and persistent conflict, posing not only a threat to the nation's peace and stability but also a substantial challenge to the international community. Moreover, Afghanistan's diverse topography, spanning mountains, deserts, and grasslands, frequently experiences natural disasters, most notably landslides. Regrettably, due to the ongoing political instability and conflict, conducting fieldwork in Afghanistan remains unfeasible at present.

3. Materials and methods

3.1. Map of landslides

Google Earth Pro (GEP) as one of the most advanced remote sensing image collection platforms, provided a large number of various high-resolution satellite images, it could be the base map for disaster interpretation (Yu and Gong, 2012). The GEP images completely covered the whole of Afghanistan, so this study used GEP exclusively as the image source for disaster interpretation. In this process, to ensure the accuracy of landslide and debris flow outlines, all interpretations were manually interpreted by a team of dozens of experienced experts, and at least two different experts cross-checked the results. We selected only images with a level larger than L18 (i.e., 0.5 m resolution) for interpretation (i.e., WorldView-2 and QuickBird satellite images with a resolution of 0.5 m in GEP). Based on the satellite imaging time, this study's disaster interpretation time range was from August 28, 2013, to September 12, 2021. ASTER GDEM V3 is used as the only digital elevation model (DEM) in the process of analyzing terrain factors such as slope and aspect due to its high accuracy and wide coverage (Abrams et al., 2020). The data sources used in this study are demonstrated in detail in Table 1.

3.2. Landslide risk assessment methodology

A complete system of landslide risk assessment includes the landslide assessment of susceptibility and hazard, as well as the vulnerability

Table 1

Data sources list. Processing of temperature, precipitation, and snow cover data see *Appendices*.

Data Types	Sources	Resolution	References
Land use type	Google Dynamic World	10 m	Brown et al. (2022)
DEM	ASTER GDEM V3	30 m	Tachikawa et al. (2011)
Satellite images	Google Earth Pro	0.5 m	/
Tectonics	U.S. Geological Survey	1:500,000	Doeblich et al. (2006)
Stratigraphic lithology			
Precipitation	Climatic Research Unit gridded Time Series	0.5° (Processing to 300 m)	Harris et al. (2020)
Temperature			
Snow cover	Science Data Bank	600 m (Processing to 300 m)	Qiu (2018)
Population	WorldPop	1 km	Tatem (2017)

assessment of the landslide-bearing body (Chang et al., 2022). Different impact factors and assessment systems are used when conducting landslide risk assessment (Dai et al., 2002). Here we briefly describe the methods and models used to conduct the risk evaluation of landslides in Afghanistan, see the *Appendices* for more information.

3.2.1. Susceptibility assessment

According to the characteristics of Afghanistan's topography and landscape, this paper divides Afghanistan into two different assessment regions: the highland assessment region and the mountain assessment region.

Based on the available literature and data, a total of ten factors were selected for susceptibility assessment in this study, namely: Slope, Aspect, Stratigraphic Lithology, Peak Ground Acceleration (PGA), Normalized Difference Vegetation Index (NDVI), Distance to road, Distance to river, Elevation, Fractional Snow Cover (FSC) and Land use type. As the highland assessment area contains more glaciers, more than half of the area is covered by snow, resulting in significant snow melt (Bishop et al., 2014). In contrast, the mountain assessment region has relatively less snow and contributes less to the occurrence of disasters. Therefore, FSC was used only in the highland assessment region, while Land use type was used only in the mountain assessment region. After a comprehensive assessment of various commonly used methods, this paper employs the FCNN to assess the susceptibility of landslides in Afghanistan. In contrast to the simpler artificial neural network with only one input layer, one hidden layer, and one output layer, our study designed an FCNN with one input layer, four hidden layers, and one output layer. This design significantly enhances model accuracy, reduces errors, and effectively avoids overfitting even with extended training time, as evidenced by the improved performance resulting from the addition of three hidden layers.

To generate random points for this study, we employed the random point generation tool in ArcGIS Pro®. The same number of random points were generated as positive and negative samples within the disaster zone and 200 m outside the disaster buffer zone, respectively (Lucchese et al., 2021; Zhou et al., 2018). The multi-value extraction to points tool in ArcGIS Pro® was used to extract the actual values of factors into each random point attribute table. Next, we marked the random points with landslide hazards as positive samples and those without landslide hazards as negative samples. The training set and validation set were randomly selected using a certain ratio, with the ratio of positive and negative samples in each set maintained at 1:1.

In the highland assessment region, this study produced 4,000 points, with and without disasters, utilizing ArcGIS Pro's random point tool and the established disaster database. The eigenvalues for the nine assessment factors were extracted using the Extract Multiple Values to Points tool and designated as positive and negative samples. From there, this

study randomly created training and validation sets for FCNN, with ratios of 8:2, 7:3, and 6:4 for the model training. In contrast, 3000 sample points each in the disaster and non-disaster areas were randomly generated in the high mountain region for the same model training. The eigenvalues of the nine factors were utilized to train the model in the highland and mountain regions. The training results revealed that when the ratio of the training and validation sets for the factors in the highland region was 7:3, the accuracy of the training results increased rapidly and the loss rate decreased swiftly. Conversely, the best model training outcomes were obtained when the ratio of the training and validation sets for the mountain region was 8:2. Therefore, this study employed two distinct ratios of training and validation sets, namely 7:3 and 8:2, for the highland and mountain regions, respectively, to predict the susceptibility of landslides for the entire area. To ensure high accuracy in the calculation of the regional model, a sequential fusion of nine factors with multi-band satellite images was performed using ArcGIS Pro®. This was followed by radiation matrix prediction at the image level, achieved with the aid of the geospatial data abstraction library (GDAL) in ArcPy® (Warmerdam, 2008). The predicted values and the susceptibility results were then returned in raster format in the form of matrix information.

3.2.2. Hazard assessment

This study integrates surface runoff and glacial snow meltwater equivalent as contributing factors, derived through the soil conservation service curve number (SCN-CN) method (Mishra et al., 2006) and Degree-day model (Braithwaite and Zhang, 2000) (See Appendices for detailed information), respectively, for risk assessment of highland and

mountain regions based on landslide susceptibility assessment. The assessment factors are subjectively weighted by AHP to assess the hazard of landslides.

3.2.3. Vulnerability assessment

This article presents a comprehensive analysis of the fundamental characteristics of landslides and their potential impact on Afghanistan. Considering the availability of assessment factors in the study area, we have developed a vulnerability assessment index system for geological hazards in Afghanistan. Specifically, we have identified five key factors, namely population density, building density, road density, and environmental vulnerability. These indicators have been carefully selected and integrated to provide a robust and accurate framework for assessing the vulnerability of regions in Afghanistan to geological hazards. This study used population density data from WorldPop (Tatem, 2017), while building and road data were obtained by manual interpretation with landslides. Land use type data were collected from Google Dynamic World (Brown et al., 2022).

The vulnerability assessment of landslide-bearing areas in Afghanistan is based on three main aspects: population vulnerability, economic vulnerability, and environmental vulnerability. Among them, the main evaluation indicator of population vulnerability is population density, the main evaluation indicator of economic vulnerability is building density and road density, and the indicator of environmental vulnerability is environmental fragility. According to existing surveys and statistical data, regions prone to landslides in Afghanistan are predominantly concentrated in major cities and towns exhibiting high population vulnerability. Although the country's average population

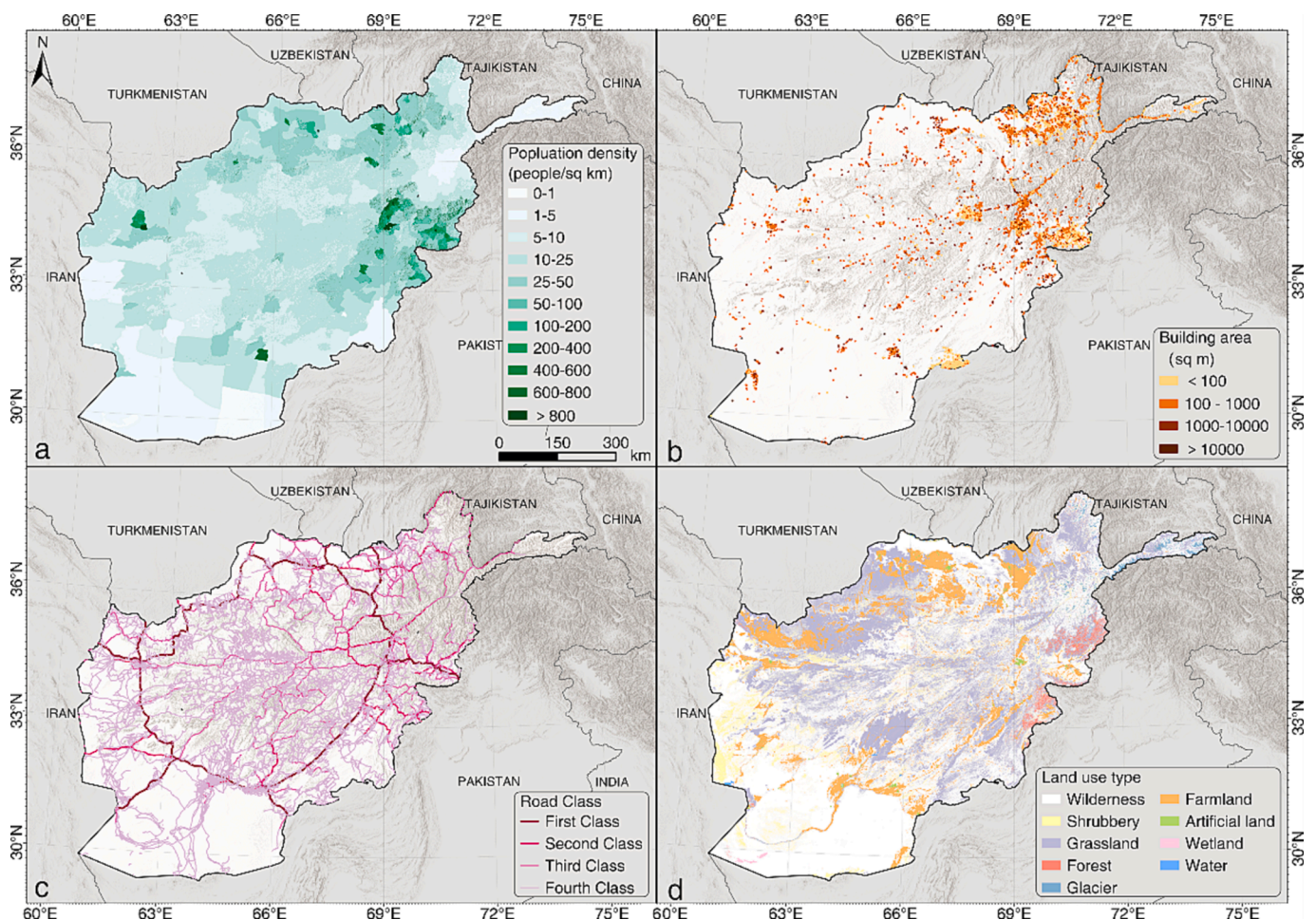


Fig. 2. Map of the distribution of different indicators: a, population density; b, building area; c, road class; d, land use type. The base map came from ESRI®.

density was a mere 49.73 people/km², Kabul, the capital, features a striking population density of approximately 1,127.29 people/km², rendering it the most densely populated city in the country. Other significant urban centers exhibit population densities between 400 and 800 people/km², while the majority of provinces and cities maintain a general population density below 200 people/km² (as shown in Fig. 2a). There were various forms of buildings as one of the disaster-bearing bodies, and the calculated normalized building density results were used to represent the vulnerability of buildings in this paper (as shown in Fig. 2b). And, owing to the results of road interpretation in Afghanistan, the roads were classified into four classes, with Class I roads suffering the most damage from landslides (as shown in Fig. 2c). In Afghanistan, the assessment of environmental vulnerability covers the environmental capacity of different land types, including arable land, woodland, scrubland, wetland, water bodies, and built-up areas, with the unit price of land factored. The findings, normalized for comparison, are illustrated in Fig. 2d.

4. Results

4.1. Distribution characteristics of landslides in Afghanistan

In this study, the interpretation covered an area of 647,500 km² and identified 3,260 landslides (as shown in Fig. 3). The results of the interpretation show that the geology of Afghanistan has a significant influence on the occurrence of landslides, most of which are of the epochal type. Areas, where bedrock is exposed, are subject to severe weathering leading to the formation of landslides. The results also show that epochal landslides tend to be medium to large in size, while recent landslides tend to be smaller.

Through statistical analysis of the distribution characteristics of landslides, it has been revealed that almost all landslides have an area of less than 1 km², of which those with an area of less than 0.1 km² have 2,620, accounting for 80.37% of the number of all landslides (as shown in Fig. 4). These catastrophic events occur in 31 out of the 34 provinces spanning Afghanistan, the specific distribution is shown in Table 2. Notably, the density of landslide occurrences is approximately 5.54 units per 1,000 km², indicating a relatively concentrated distribution. Furthermore, among the provinces experiencing landslide events,

Badakhshan, Parwan, Samangan and Takhar Provinces stand out as areas with a high density, with values surpassing 10 units per 1,000 km².

4.2. Landslide susceptibility assessment result

The assessment result of landslide susceptibility in the highland and mountain regions is shown in Fig. 5 and Table 3. Specifically, in the highland region, 9.239 % of all assessed zones exhibited high susceptibility, with medium and low susceptibility accounting for 12.96% and 21.23%, respectively. In the mountain region, 5.30% of the assessed zones were categorized as highly susceptible to landslides, while 3.30% and 4.61% were classified as medium and low susceptibility, respectively, with the remaining 86.94% being deemed less prone to landslides. Combined with the topographic and geomorphological features of Afghanistan, the high landslide susceptibility zones are mainly located in regions with steep terrain and more abundant physical sources. The highland region has a much higher susceptibility to landslides compared to the mountain region.

4.3. Landslide hazard assessment result

Using the discriminant matrix from the AHP, we analyzed the meltwater equivalent and surface runoff and derived hazard weight matrices for the highland and mountain regions as shown in Table 4 and Table 5. Using the results of the meltwater equivalent, surface runoff, and susceptibility, we performed an overlay analysis in ArcGIS Pro ® to derive the landslide hazard assessments.

The calculated results were classified into low, medium, high, and very high hazard zones using the reclassification tool of ArcGIS Pro ® with the natural breakpoint method (Nandi and Shakoor, 2008), following the principle of landslide hazard increasing from small to large. The hazard assessment results were analyzed separately for the highland and mountain regions (as shown in Fig. 6 and Table 6). And the results showed that in the highland region, the total area of landslide hazard assessment is 9,6281.53 km², with 9,558.51 km² (9.93% of the total area) classified as very high hazard zone, 13,001.35 km² (13.50% of the total area) classified as high hazard zone, and 21,241.31 km² (22.06% of the total area) classified as a medium hazard zone. In the mountain region, the total area of landslide hazard assessment is

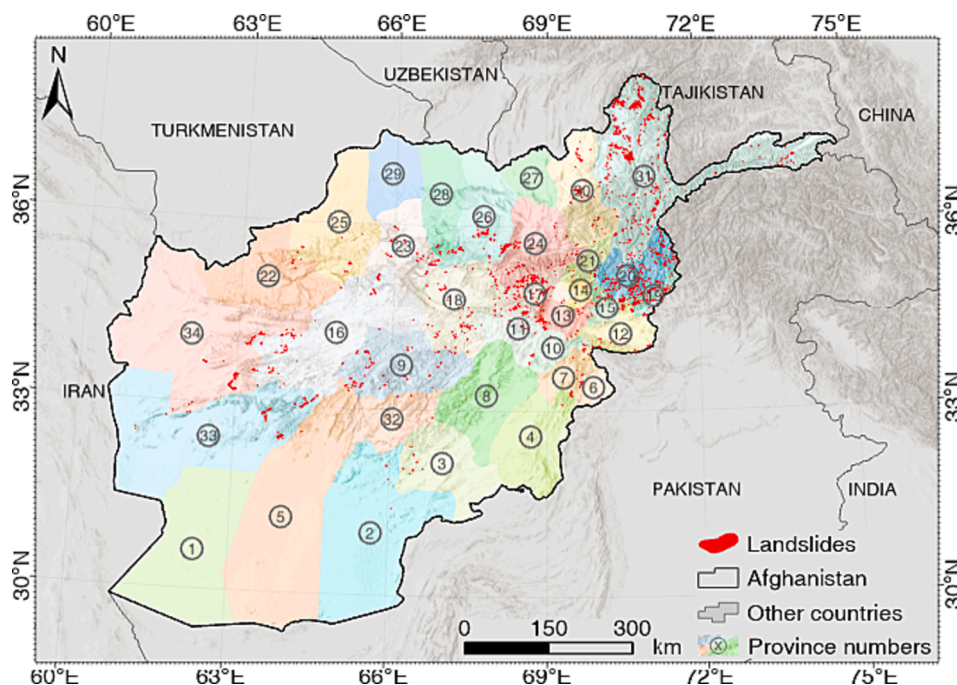


Fig. 3. Map of landslide distribution for Afghanistan.

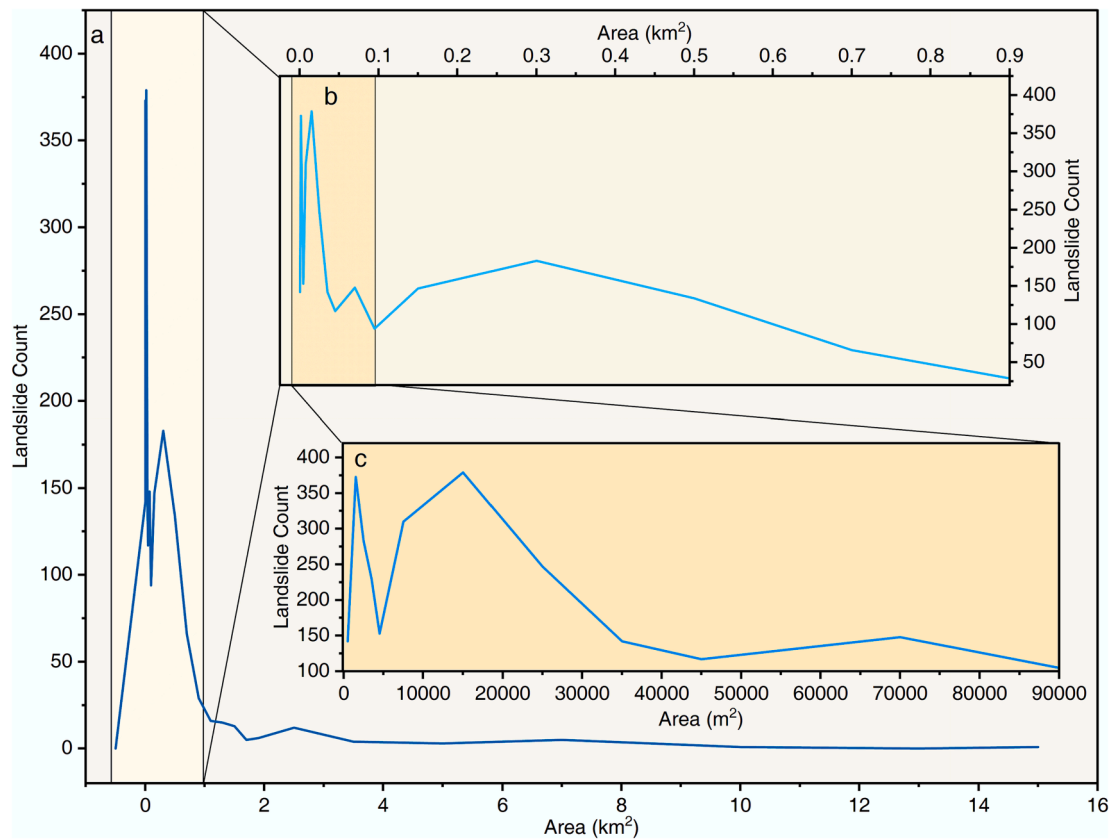


Fig. 4. Frequency statistics for landslide area: (a) for all areas, (b) for landslides less than 1 km², and (c) for landslides less than 0.09 km².

Table 2
Density of landslide distribution in various provinces of Afghanistan.

Numbers	Province	Area of Province (km ²)	Landslide Counts	Density of Landslides (units/1000 km ²)
2	Kunduz	44756.55	4	0.09
3	Zabul	18550.75	25	1.35
4	Paktika	19643.32	12	0.61
5	Helmand	54984.86	18	0.33
6	Khost	3443.88	17	4.94
7	Paktia	5544.37	18	3.25
8	Ghazni	20514.34	1	0.05
9	Daykundi	20999.85	128	6.10
10	Logar	4554.90	24	5.27
11	Wardak	7489.32	90	12.02
12	Nangarhar	7902.99	71	8.98
13	Kabul	4829.14	51	10.56
14	Kapisa	2398.59	7	2.92
15	Laghman	3139.19	59	18.79
16	Ghazni	34213.73	139	4.06
17	Parwan	5922.47	194	32.76
18	Bamyan	19750.15	149	7.54
19	Kunar	3136.62	164	52.29
20	Nuristan	11452.45	312	27.24
21	Panjshir	3621.91	15	4.14
22	Badghis	24541.79	19	0.77
23	Sar-e-Pol	14144.20	74	5.23
24	Baghlan	16401.87	142	8.66
25	Faryab	24938.11	25	1.00
26	Samangan	17972.35	176	9.79
28	Balkh	13997.23	17	1.21
30	Takhar	16776.30	71	4.23
31	Badakhshan	47319.72	854	18.05
32	Uruzgan	11935.11	3	0.25
33	Farah	49782.69	146	2.93
34	Herat	53852.58	235	4.36

293,247.38 km², with 15,862.640 km² (5.41% of the total area) classified as a very high hazard zone, 28,564.74 km² (9.74% of the total area) classified as high hazard zone, and 30,214.95 km² (10.30% of the total area) classified as a medium hazard zone. As with the susceptibility results, these findings suggested that the hazard of landslides is significantly higher in the highland region than in the mountain region.

4.4. Vulnerability assessment of the bearing area

The holistic vulnerability assessment of landslides in Afghanistan was derived by considering the aforementioned evaluation factors (as shown in Table 7, Table 8, and Fig. 7). High and very high vulnerability zones predominantly occurred in regions with dense populations, well-developed infrastructure, including housing, and extensive surface arable land. These zones were chiefly found in the central and western provinces surrounding the capital city, as well as in the northern provinces of Afghanistan. Characterized by low-lying terrain and relatively advanced transportation systems, these zones are conducive to agricultural production and human settlement. Consequently, the probability of human casualties and economic losses due to landslides was elevated, with significant potential impacts. Furthermore, high vulnerability zones could also be found in other mountainous and gully locations where larger flat expanses are present. The medium vulnerability zones were distributed around the high susceptibility zones.

4.5. Landslide risk assessment result

Landslide risk assessment in Afghanistan was conducted through matrix analysis, as depicted in Fig. 8. Owing to the reduced likelihood of landslide occurrences in areas with low susceptibility, the associated risk in these zones was determined to be low. The outcomes of the risk assessment revealed a distinct spatial pattern in the distribution of landslide risks across Afghanistan (as shown in Fig. 9 and Table 9). Very

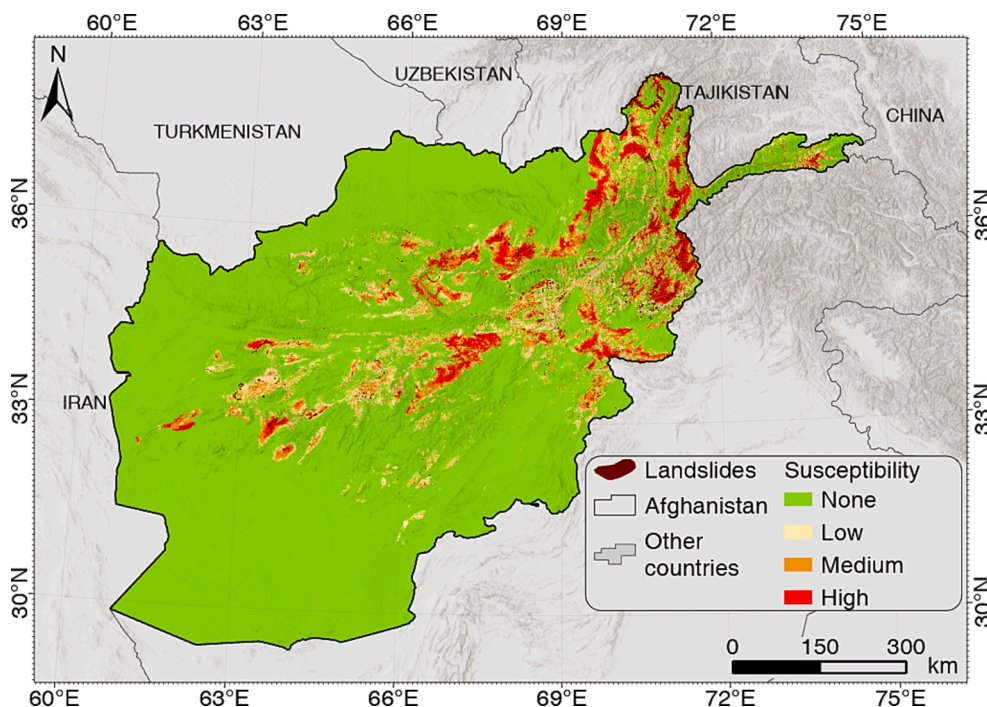


Fig. 5. Distribution map of landslide susceptibility assessment.

Table 3
Landslide susceptibility statistics for highland and mountain regions.

Region	Class	Landslide Area (km ²)	Landslide area as a percentage (%)	Landslide density
Highland	None	1.44	0.50	0.0274 × 10 ⁻³
	Low	8.52	2.95	0.4328 × 10 ⁻³
	Medium	30.73	10.64	2.3304 × 10 ⁻³
	High	248.00	85.91	22.832 × 10 ⁻³
Mountain	None	0.06	0.09	0.0002 × 10 ⁻³
	Low	0.06	0.09	0.0043 × 10 ⁻³
	Medium	0.23	0.35	0.0241 × 10 ⁻³
	High	66.76	99.48	4.3001 × 10 ⁻³

Table 4
Hazard weighting discriminant matrix for the highland region.

Factor	Susceptibility	Meltwater equivalent	Surface runoff	Weight
Susceptibility	1	4	5	0.6648
Meltwater equivalent	1/4	1	4	0.2449
Surface runoff	1/5	1/4	1	0.0902

high and high risk zones are mainly located in the tectonically developed areas along the Hindu Kush, especially along the Kolcha River that straddles the border between Takhar and Badakhshan Provinces. Other high-risk areas include the Kabul River along the border of Nangarhar, Laghman, Kapisa and Kabul Provinces. In addition, these risk-prone areas are also concentrated along the Helmand River as well as along the Hindu Kush, and are evident in the traffic-developed areas of

Table 5
Hazard weighting discriminant matrix for the mountain region.

Factor	Susceptibility	Surface runoff	Meltwater equivalent	Weight
Susceptibility	1	5	6	0.7016
Surface runoff	1/5	1	5	0.2258
Meltwater equivalent	1/6	1/5	1	0.0727

Nuristan, Khulna, Nangarhar, Logar, Khost, Farah, and Baghlan Provinces, as well as scattered in the Hindu Kush areas along the route. Zones of medium risk were more uniformly distributed across Afghanistan, predominantly in the eastern region of the country. Due to these zones primarily comprised high mountainous and valley terrain, the population distribution is comparatively concentrated and susceptible to disaster-related losses. Notably, Kabul, Panjshir, Nangarhar, and Badakhshan provinces represented the most conspicuous medium risk zones within the territory. Additionally, Kandahar and Uruzgan provinces in southern Afghanistan, as well as the western regions of Herat province, which were situated near the periphery of population agglomerations, also fell within the medium-risk classification.

5. Conclusions and discussion

As a country susceptible to seismic events, co-seismic and post-seismic landslides crucially imperil human life and property of Afghanistan. However, the prevailing uncertainty caused by conflict and other unavoidable reasons made fieldwork remain infeasible. In this study, we have successfully established the first-ever landslide inventory utilizing optical satellite imagery and manual visual interpretation. This inventory mapped 3,260 landslides covering the whole of Afghanistan from 2015 to the present. Most of them are distributed in the north-eastern mountainous region. Based on this inventory, we conducted a detailed risk assessment including landslide susceptibility and hazard, and vulnerability of the bearing area. Given the country's unique geographical location and climate, we integrated hazard assessment results with two factors—meltwater equivalent from glaciers and snow

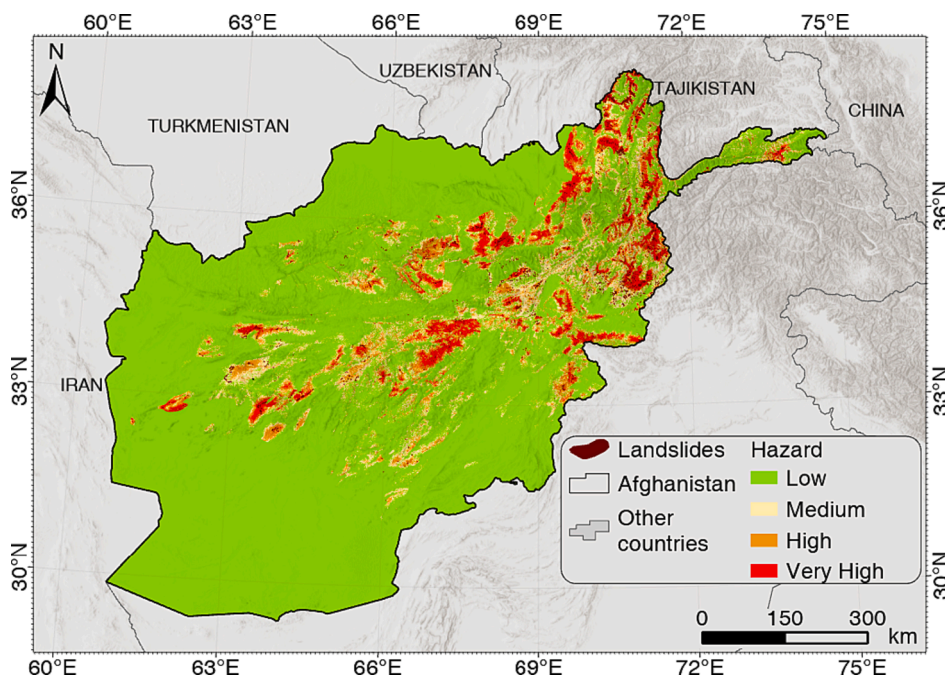


Fig. 6. Hazard assessment distribution map of landslide in Afghanistan.

Table 6
Landslide hazard statistics for highland and mountain regions.

Region	Class	Landslide Area (km ²)	Landslide area as a percentage (%)	Disaster density
Highland	Low	3.57	1.24	0.0728×10^{-3}
	Medium	11.39	3.95	0.5087×10^{-3}
	High	34.70	12.02	2.4133×10^{-3}
	Very high	239.09	82.80	22.750×10^{-3}
Mountain	Low	0.06	0.09	0.0002×10^{-3}
	Medium	0.12	0.18	0.0071×10^{-3}
	High	0.47	0.69	0.0447×10^{-3}
	Very high	66.65	99.05	4.2382×10^{-3}

and surface runoff—to evaluate landslide hazards in Afghanistan. We found a large number of very high and high risk zones in the tectonically developed areas along the Hindu Kush, as well as many medium risk regions in the more populated areas of eastern Afghanistan.

Compared with previous studies of landslides in Afghanistan, we adopted two distinct geographic settings, namely highland and mountain regions. In this way, we conducted the assessment of the whole of Afghanistan rather than some specific mountainous or watershed

Table 7
Factor weights, CR and λ_{max} of the AHP matrix for vulnerability evaluation. Here, CR is the stochastic consistency ratio of the matrix; λ_{max} is the maximum eigenvalue of the matrix.

Factor	Population density	Building density	Road density	Environmental vulnerability	Weight	CR	λ_{max}
Population density	1	3	4	5	0.4258	0.0079	3.0092
Building density	1/3	1	3	4	0.2945		
Road density	1/4	1/2	1	3	0.1848		
Environmental vulnerability	1/5	1/4	1/3	1	0.0949		

regions. In the research by Zhang et al. (2015), an extensive analysis was undertaken concerning the Abe Berek landslide, a significant event that transpired on May 2, 2014, within the confines of Badakhshan Province, Afghanistan. Employing the weight-of-evidence methodology, Zhang et al. (2015) meticulously conducted a susceptibility assessment that encompassed a substantial 609 landslides across the region. In this study, we mapped 854 landslides within Badakhshan province, which served as a complement to Zhang et al.’s map, particularly in the unexplored regions of Wakhan and other adjacent areas. An insightful comparison of our findings with Zhang et al.’s results within overlapping mapped landslide-prone. This compelling congruence substantiates the methodological soundness underpinning our assessment and, by extension, attests to the scientific validity and reliability of the outcomes

Table 8
Landslide vulnerability statistics for highland and mountain regions.

Region	Class	Graded raster counts	Graded Area (km ²)	Graded area as a percentage (%)
Highland	Low	834,415	52555.905	54.586
	Medium	514,322	32394.752	33.646
	High	124,485	7840.687	8.144
	Very high	55,413	3490.186	3.625
Mountain	Low	2,083,431	130353.349	44.452
	Medium	1,744,788	109165.583	37.226
	High	746,103	46681.184	15.919
	Very high	112,636	7047.260	2.403

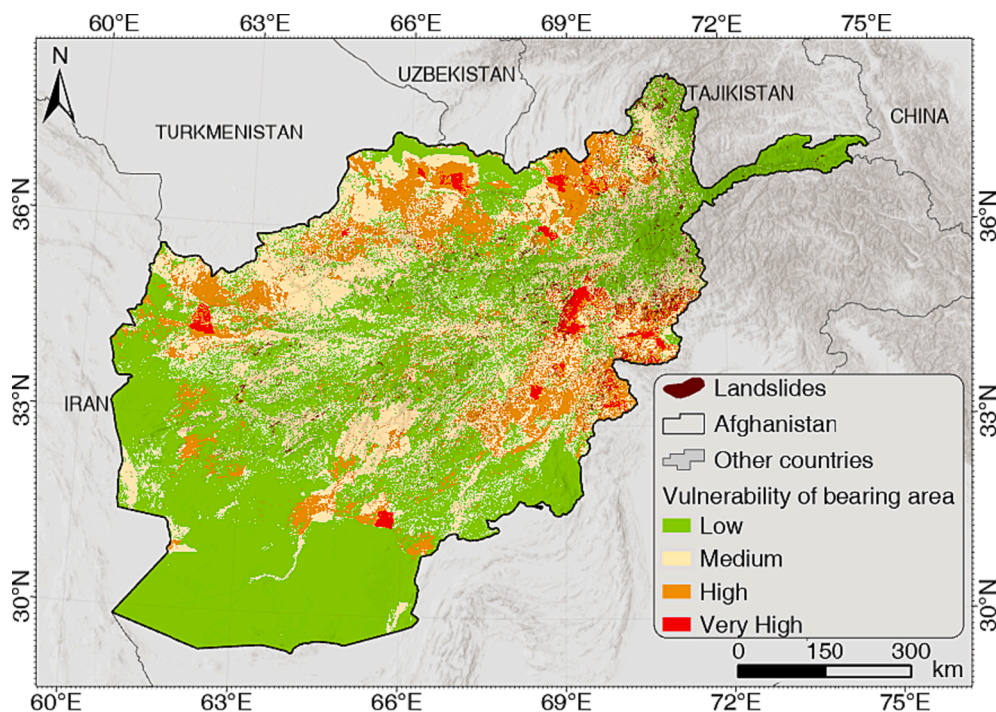


Fig. 7. Vulnerability assessment of landslide-bearing area for highland and mountain regions.

Vulnerability \ Hazard	Risk			
	Very high	High	Medium	Low
Very high	Very high	Very high	High	Medium
High	Very high	High	Medium	Medium
Medium	High	High	Medium	Low
Low	High	Medium	Low	Low

Fig. 8. Landslide risk rating matrix for Afghanistan.

presented herein. Furthermore, during the concluding manual inspection phase of our landslide inventory, we extensively cross-referenced the previously documented landslides by Shroder et al. (2011a, b). While Shroder et al.'s research primarily focused on elucidating the mechanisms and characteristics of these landslides without delving into a comprehensive risk assessment, their work nonetheless furnished a robust underpinning for landslide validation within the purview of this study.

While this study has effectively mapped landslides across Afghanistan from 2015 to the present, an obvious constraint lies in our inability to undertake on-site field surveys to the identified landslides and access to detailed local population and building. The absence of such field surveys represents a primary limitation of this study endeavor. These field investigations are essential for rigorously validating the

accuracy of our mapping outcomes and furnishing data for refining the selection and weighting of factors involved in landslide risk assessment. This also could promise to enhance the precision and reliability of our evaluation results. Besides, Afghanistan is also confronted with other hazards, including rock avalanches, debris flows, glacial lake outburst floods, and others. These additional hazards will be the primary focus of our subsequent research efforts.

In conclusion, for Afghanistan, detailed monitoring and early warning of existing landslides is particularly important. This study provides a detailed checklist and guidelines for the Government of Afghanistan to carry out landslide monitoring and early warning. Installation of the necessary monitoring equipment in key areas close to cities to observe the stability of slopes promptly. Disaster awareness in remote and underdeveloped areas should be promoted through

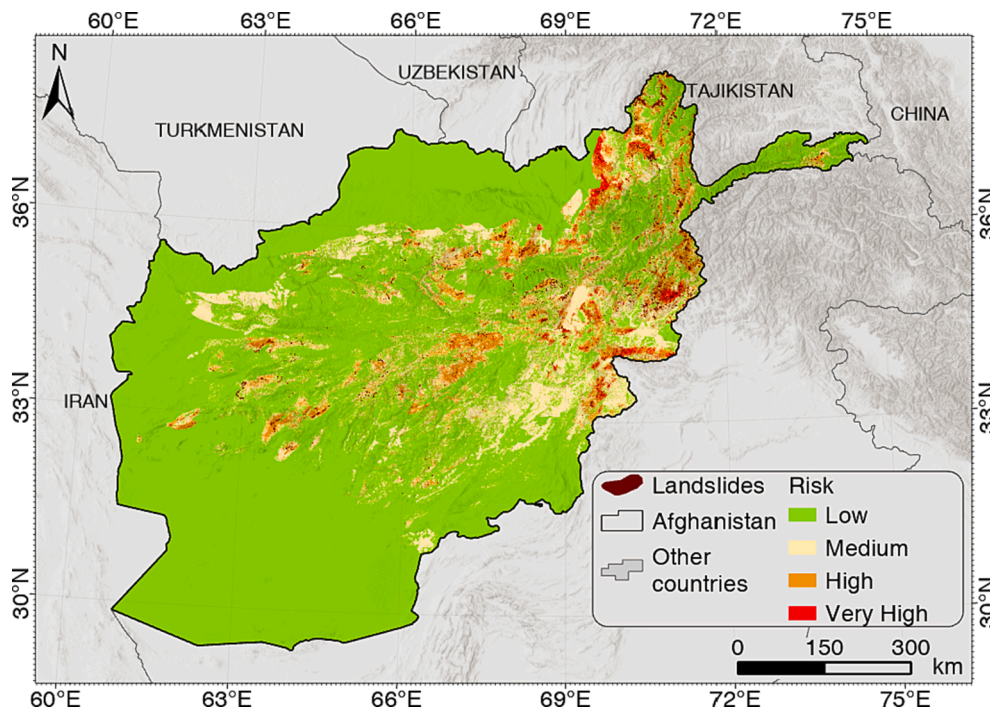


Fig. 9. Risk assessment distribution of landslide in Afghanistan.

Table 9
Landslide risk statistics for Afghanistan.

Risk Class	Landslide raster counts	Landslide Area (km ²)	Landslide area as a percentage (%)	Disaster density
Low	93	5.80	1.63	0.0103 × 10 ⁻³
Medium	1411	88.04	24.67	1.4226 × 10 ⁻³
High	3612	225.38	63.15	11.577 × 10 ⁻³
Very high	604	37.68	10.55	10.478 × 10 ⁻³

extensive publicity and training to ensure that people can notice impending landslides and take effective evacuation measures. Furthermore, we anticipate that the ongoing advancements in satellite technology will usher in a new era of higher-resolution imagery. This holds the potential to address the existing shortcomings in our current dataset, thereby bolstering the comprehensiveness and efficacy of our landslide assessments.

CRedit authorship contribution statement

Ming Chang: Conceptualization, Writing – original draft, Writing – review & editing, Project administration, Resources, Funding acquisition. **Xiangyang Dou:** Conceptualization, Methodology, Formal analysis, Visualization, Writing – original draft, Writing – review & editing. **Fenghuan Su:** Writing – review & editing, Resources, Funding acquisition. **Bo Yu:** Methodology, Software, Data curation, Formal analysis.

Declaration of Competing Interest

The authors declare that they have no known competing financial interests or personal relationships that could have appeared to influence the work reported in this paper.

Data availability

Data will be made available on request.

Acknowledgments

This research was financially supported by the Second Tibetan Plateau Scientific Expedition and Research Program (STEP) (grant number 2019QZKK0902), the National Natural Science Foundation of China (grant number 42077245), and the State Key Laboratory of Geohazard Prevention and Geoenvironment Protection Independent Research Project (grant number SKLGP2022Z005). Xiangyang Dou would like to thank the China Scholarship Council (CSC) for funding his research period at the University of Twente (grant number 202309230008). The authors acknowledge the constructive comments from the editor and reviewers improving the quality of this manuscript.

Appendix A. Supplementary data

Supplementary data to this article can be found online at <https://doi.org/10.1016/j.ecolind.2023.111179>.

References

Abrams, M., Crippen, R., Fujisada, H., 2020. ASTER Global Digital Elevation Model (GDEM) and ASTER Global Water Body Dataset (ASTWBD). *Remote Sens.-Basel* 12 (7), 1156. <https://doi.org/10.3390/rs12071156>.
 Agung, P.A., Maha, H., Rouf, M.F., Susilo, A., Ahmad, M.A., Ahmad, B., Mohd, J., Abdurrahman, U.A., Sudjianto, A.T., Suryo, E.A., 2023. Compilation of parameter control for mapping the potential landslide areas. *Civil Eng. J.* 9 (4), 974–989. <https://doi.org/10.28991/cej-2023-09-04-016>.
 Aliyar, Q., Esmailnejad, M., 2022. Assessment of the change of trend in precipitation over Afghanistan in 1979–2019. *IDŐJÁRÁS/Q. J. Hungary. Meteorol. Serv.* 126 (2), 185–201.
 Bishop, M.P., Shroder, J.F., Ali, G., Bush, A.B.G., Haritashya, U.K., Roohi, R., Sarikaya, M.A., Weihs, B.J., 2014. In: *Global Land Ice Measurements from Space*. Springer Berlin Heidelberg, Berlin, Heidelberg, pp. 509–548.
 Boyd, O.S., Mueller, C.S., Rukstales, K.S., 2007. Preliminary earthquake hazard map of Afghanistan. *U.S. Geol. Surv. Open File Rep.*, p. 1137.
 Braithwaite, R.J., Zhang, Y., 2000. Sensitivity of mass balance of five Swiss glaciers to temperature changes assessed by tuning a degree-day model. *J. Glaciol.* 46 (152), 7–14. <https://doi.org/10.3189/172756500781833511>.

- Brown, C.F., Brumby, S.P., Guzder-Williams, B., Birch, T., Hyde, S.B., Mazzariello, J., Czerwinski, W., Pasquarella, V.J., Haertel, R., Ilyushchenko, S., Schwehr, K., Weisse, M., Stolle, F., Hanson, C., Guinan, O., Moore, R., Tait, A.M., 2022. Dynamic World, Near real-time global 10 m land use land cover mapping. *Sci. Data* 9 (1), 251. <https://doi.org/10.1038/s41597-022-01307-4>.
- Casagli, N., Intrieri, E., Tofani, V., Gigli, G., Raspini, F., 2023. Landslide detection, monitoring and prediction with remote-sensing techniques. *Nat. Rev. Earth Environ.* 4 (1), 51–64. <https://doi.org/10.1038/s43017-022-00373-x>.
- Causes, L., 2001. *Landslide Types and Processes*. US Geological Survey, Reston, VA, USA.
- Chang, M., Dou, X., Hales, T.C., Yu, B., 2021. Patterns of rainfall-threshold for debris-flow occurrence in the Wenchuan seismic region, Southwest China. *Bull. Eng. Geol. Environ.* 80 (3), 2117–2130. <https://doi.org/10.1007/s10064-020-02080-7>.
- Chang, M., Dou, X., Tang, L., Xu, H., 2022. Risk assessment of multi-disaster in Mining Area of Guizhou, China. *Int. J. Disast. Risk Res.* 78, 103128.
- Chen, L.F., Guo, H.X., Gong, P.S., Yang, Y.Y., Zuo, Z.L., Gu, M.Y., 2021. Landslide susceptibility assessment using weights-of-evidence model and cluster analysis along the highways in the Hubei section of the Three Gorges Reservoir Area. *Comput. Geosci-Uk* 156, 104899. <https://doi.org/10.1016/j.cageo.2021.104899>.
- Chomba, I.C., Banda, K.E., Winsemius, H.C., Eunice, M., Sichingabula, H.M., Nyambe, I. A., 2022. Integrated hydrologic-hydrodynamic inundation modeling in a groundwater dependent tropical floodplain. *J. Hum. Earth Future* 3 (2), 237–246. <https://doi.org/10.28991/hef-2022-03-02-09>.
- Cui, P., Zhu, Y.Y., Han, Y.S., Chen, X.Q., Zhuang, J.Q., 2009. The 12 May Wenchuan earthquake-induced landslide lakes: distribution and preliminary risk evaluation. *Landslides* 6 (3), 209–223. <https://doi.org/10.1007/s10346-009-0160-9>.
- Cui, P., Dang, C., Zhuang, J.Q., You, Y., Chen, X.Q., Scott, K.M., 2012. Landslide-dammed lake at Tangjiashan, Sichuan province, China (triggered by the Wenchuan Earthquake, May 12, 2008): risk assessment, mitigation strategy, and lessons learned. *Environ. Earth Sci.* 65 (4), 1055–1065. <https://doi.org/10.1007/s12665-010-0749-2>.
- Dai, Y.Q., Bai, X.F., Nie, G.Z., Huangfu, G., 2022. A rapid assessment method for earthquake-induced landslide casualties based on GIS and logistic regression model*. *Geomat. Nat. Haz. Risk* 13 (1), 222–248. <https://doi.org/10.1080/19475705.2021.2017022>.
- Dai, F.C., Lee, C.F., Ngai, Y.Y., 2002. Landslide risk assessment and management: an overview. *Eng. Geol.* 64 (1), 65–87. [https://doi.org/10.1016/S0013-7952\(01\)00093-X](https://doi.org/10.1016/S0013-7952(01)00093-X).
- Do, H.M., Yin, K.L., Guo, Z.Z., 2020. A comparative study on the integrative ability of the analytical hierarchy process, weights of evidence and logistic regression methods with the Flow-R model for landslide susceptibility assessment. *Geomat. Nat. Haz. Risk* 11 (1), 2449–2485. <https://doi.org/10.1080/19475705.2020.1846086>.
- Doeblich, J.L., Wahl, R.R., Ludington, S.D., Chirico, P.G., Wandrey, C.J., Bohannon, R.G., Orris, G.J., Bliss, J.D., 2006. *Geologic Age and Lithology of Afghanistan (glgafg.shp)*, U.S. Geological Survey - ScienceBase [data set], <https://doi.org/10.5066/P9013L2C>, (last access: 1 June 2023).
- Dou, X., Fan, X., Wang, X., Yunus, A.P., Xiong, J., Tang, R., Lovati, M., van Westen, C., Xu, Q., 2023. Spatio-temporal evolution of glacial lakes in the Tibetan Plateau over the past 30 years. *Remote Sens.-Basel* 15 (2), 416. <https://doi.org/10.3390/rs15020416>.
- Fan, X., Wang, X., Dai, L., Fang, C., Deng, Y., Zou, C., Tang, M., Wei, Z., Dou, X., Zhang, J., 2022. Characteristics and spatial distribution pattern of M S 6.8 Luding earthquake occurred on September 5, 2022. *J. Eng. Geol.*, 30(5), 1504–1516. <https://doi.org/10.13544/j.cnki.jeg.2022-0665>.
- Fan, X.M., Scaringi, G., Xu, Q., Zhan, W.W., Dai, L.X., Li, Y.S., Pei, X.J., Yang, Q., Huang, R.Q., 2018. Coseismic landslides triggered by the 8th August 2017 M-s 7.0 Jiuzhaigou earthquake (Sichuan, China): factors controlling their spatial distribution and implications for the seismogenic blind fault identification. *Landslides* 15 (5), 967–983. <https://doi.org/10.1007/s10346-018-0960-x>.
- Fan, X., Scaringi, G., Domènech, G., Yang, F., Guo, X., Dai, L., He, C., Xu, Q., Huang, R., 2019a. Two multi-temporal datasets that track the enhanced landslide after the 2008 Wenchuan earthquake. *Earth Syst. Sci. Data* 11 (1), 35–55. <https://doi.org/10.5194/essd-11-35-2019>.
- Fan, X., Scaringi, G., Korup, O., West, A.J., van Westen, C.J., Tanyas, H., Hovius, N., Hales, T.C., Jibson, R.W., Allstadt, K.E., Zhang, L., Evans, S.G., Xu, C., Li, G., Pei, X., Xu, Q., Huang, R., 2019b. Earthquake-induced chains of geologic hazards: patterns, mechanisms, and impacts. *Rev. Geophys.* 57 (2), 421–503. <https://doi.org/10.1029/2018rg000626>.
- Gao, Z.M., Ding, M.T., 2022. Application of convolutional neural network fused with machine learning modeling framework for geospatial comparative analysis of landslide susceptibility. *Nat. Hazards* 113 (2), 833–858. <https://doi.org/10.1007/s11069-022-05326-7>.
- Gariano, S.L., Guzzetti, F., 2016. Landslides in a changing climate. *Earth Sci. Rev.* 162, 227–252. <https://doi.org/10.1016/j.earscirev.2016.08.011>.
- Glade, T., 2003. Vulnerability assessment in landslide risk analysis. *Erde* 134 (2), 123–146.
- Haritashya, U.K., Bishop, M.P., Shroder, J.F., Bush, A.B.G., Bulley, H.N.N., 2009. Space-based assessment of glacier fluctuations in the Wakhan Pamir, Afghanistan. *Clim. Change* 94 (1–2), 5–18. <https://doi.org/10.1007/s10584-009-9555-9>.
- Harris, I., Osborn, T.J., Jones, P., Lister, D., 2020. Version 4 of the CRU TS monthly high-resolution gridded multivariate climate dataset. *Sci. Data* 7 (1), 109. <https://doi.org/10.1038/s41597-020-0453-3>.
- Huang, R., Fan, X., 2013. The landslide story. *Nat. Geosci.* 6 (5), 325–326.
- Huang, F.M., Zhang, J., Zhou, C.B., Wang, Y.H., Huang, J.S., Zhu, L., 2020. A deep learning algorithm using a fully connected sparse autoencoder neural network for landslide susceptibility prediction. *Landslides* 17 (1), 217–229. <https://doi.org/10.1007/s10346-019-01274-9>.
- Joya, E., Bromand, M.T., Murtaza, K.O., Dar, R.A., 2021. Current glacier status and ELA changes since the Late Pleistocene in the Hindu Kush Mountains of Afghanistan. *J. Asian Earth Sci.* 219, 104897. <https://doi.org/10.1016/j.jseas.2021.104897>.
- Kayastha, P., Dhital, M.R., De Smedt, F., 2013. Application of the analytical hierarchy process (AHP) for landslide susceptibility mapping: A case study from the Tinau watershed, west Nepal. *Comput. Geosci-Uk* 52, 398–408. <https://doi.org/10.1016/j.cageo.2012.11.003>.
- Lin, C.-W., Liu, S.-H., Lee, S.-Y., Liu, C.-C., 2006. Impacts of the Chi-Chi earthquake on subsequent rainfall-induced landslides in central Taiwan. *Eng. Geol.* 86 (2–3), 87–101. <https://doi.org/10.1016/j.enggeo.2006.02.010>.
- Lucchese, L.V., de Oliveira, G.G., Pedrollo, O.C., 2021. Investigation of the influence of nonoccurrence sampling on landslide susceptibility assessment using Artificial Neural Networks. *Catena* 198, 105067. <https://doi.org/10.1016/j.catena.2020.105067>.
- Menon, A., Lai, C.G., Macchi, G., 2004. Seismic hazard assessment of the historical site of Jam in Afghanistan and stability analysis of the minaret. *J. Earthq.* 8 (sup001), 251–294.
- Mishra, S.K., Tyagi, J.V., Singh, V.P., Singh, R., 2006. SCS-CN-based modeling of sediment yield. *J. Hydrol.* 324 (1–4), 301–322. <https://doi.org/10.1016/j.jhydrol.2005.10.006>.
- Nandi, A., Shakoor, A., 2008. Application of logistic regression model for slope instability prediction in Cuyahoga River watershed, Ohio, USA. *Georisk* 2 (1), 16–27. <https://doi.org/10.1080/17499510701842221%20Taylor%20Francis>.
- Qiu, Y., 2018. Daily fractional snow cover dataset over High Asia (2002–2016), A Big Earth Data Platform for Three Poles [data set], <https://doi.org/10.11888/GlaciolGeoctrlpe.0000016.file>, (last access: 1 June 2023).
- Rosly, M.H., Mohamad, H.M., Bolong, N., Harith, Herayani, N.S., 2023. Relationship of Rainfall Intensity with Slope Stability. *Civil Engineering Journal* 9, 75–82. <https://doi.org/10.28991/cej-sp2023-09-06>.
- Rousta, I., Olafsson, H., Moniruzzaman, M.d., Zhang, H., Liou, Y.-A., Mushore, T.D., Gupta, A., 2020. Impacts of drought on vegetation assessed by vegetation indices and meteorological factors in Afghanistan. *Remote Sens. (Basel)* 12 (15), 2433.
- Shahabi, H., Khezri, S., Bin Ahmad, B., Hashim, M., 2022. Landslide susceptibility mapping at central Zab basin, Iran: A comparison between analytical hierarchy process, frequency ratio and logistic regression models. *Catena* 208. <https://doi.org/10.1016/j.catena.2021.105784>.
- Shahi, D.K., 2022. Afghanistan and its neighbourhood challenges and opportunities of international interaction. *Asian J. Res. Soc. Sci. Human.* 12 (6), 106–118.
- Shroder, J.F., Schettler, M.J., Weihs, B.J., 2011a. Loess failure in northeast Afghanistan. *Phys. Chem. Earth, Parts A/B/C* 36 (16), 1287–1293.
- Shroder, J.F., Weihs, B.J., Schettler, M.J., 2011b. Mass movement in northeast Afghanistan. *Phys. Chem. Earth, Parts A/B/C* 36 (16), 1267–1286.
- Shroder, J.F., Eqrar, N., Waizy, H., Ahmadi, H., Weihs, B.J., 2022. Review of the Geology of Afghanistan and its water resources. *Int. Geol. Rev.* 64 (7), 1009–1031.
- Tachikawa, T., Hato, M., Kaku, M., Iwasaki, A., 2011. Characteristics of ASTER GDEM version 2. In: 2011 IEEE International Geoscience and Remote Sensing Symposium. IEEE, pp. 3657–3660.
- Tan, Y.M., Guo, D., Xu, B., 2015. A geospatial information quantity model for regional landslide risk assessment. *Nat. Hazards* 79 (2), 1385–1398. <https://doi.org/10.1007/s11069-015-1909-1>.
- Tatem, A.J., 2017. Comment: WorldPop, open data for spatial demography. *Sci. Data* 4, 170004. <https://doi.org/10.1038/sdata.2017.4>.
- Vaidya, O.S., Kumar, S., 2006. Analytic hierarchy process: An overview of applications. *Eur. J. Oper. Res.* 169 (1), 1–29. <https://doi.org/10.1016/j.ejor.2004.04.028>.
- van Westen, C.J., Castellanos, E., Kuriakose, S.L., 2008. Spatial data for landslide susceptibility, hazard, and vulnerability assessment: An overview. *Eng. Geol.* 102 (3–4), 112–131. <https://doi.org/10.1016/j.enggeo.2008.03.010>.
- Wang, X., Fang, C., Tang, X., Dai, L., Fan, X., Xu, Q., 2022. Research on emergency evaluation of landslides induced by Luding Ms 6.8 earthquake. *Geomatics and Information Science of Wuhan University*.
- Warmerdam, F., 2008. The geospatial data abstraction library. In: Hall, G.B., Leahy, M.G. (Eds.), *Advances in Geographic Information Science/Open Source Approaches in Spatial Data Handling*. Springer Berlin Heidelberg, Berlin, Heidelberg, pp. 87–104.
- Waseem, M., Lateef, A., Ahmad, I., Khan, S., Ahmed, W., 2018. Seismic hazard assessment of Afghanistan. *J. Seismol.* 23 (2), 217–242. <https://doi.org/10.1007/s10950-018-9802-5>.
- Yu, L.e., Gong, P., 2012. Google Earth as a virtual globe tool for Earth science applications at the global scale: progress and perspectives. *Int. J. Remote Sens.* 33 (12), 3966–3986.
- Yuan, X., Liu, C., Nie, R., Yang, Z., Li, W., Dai, X., Cheng, J., Zhang, J., Ma, L., Fu, X., Tang, M., Xu, Y., Lu, H., 2022. A comparative analysis of certainty factor-based machine learning methods for collapse and landslide susceptibility mapping in Wenchuan County, China. *Remote Sens. (Basel)* 14 (14), 3259. <https://doi.org/10.3390/rs14143259>.
- Zhang, T.Y., Fu, Q., Li, C., Liu, F.F., Wang, H.Y., Han, L., Quevedo, R.P., Chen, T.Q., Lei, N., 2022. Modeling landslide susceptibility using data mining techniques of kernel logistic regression, fuzzy unordered rule induction algorithm, SysFor and random forest. *Nat. Hazards* 114 (3), 3327–3358. <https://doi.org/10.1007/s11069-022-05520-7>.
- Zhang, J., Gurung, D.R., Liu, R., Murthy, M., Ramachandra, M.S., Su, F., 2015. Abe Berek landslide and landslide susceptibility assessment in Badakhshan Province, Afghanistan. *Landslides* 12 (3), 597–609. <https://doi.org/10.1007/s10346-015-0558-5>.
- Zhou, C., Yin, K.L., Cao, Y., Ahmed, B., Li, Y.Y., Catani, F., Pourghasemi, H.R., 2018. Landslide susceptibility modeling applying machine learning methods: A case study

from Longju in the Three Gorges Reservoir area, China. *Comput. Geosci.-Uk* 112, 23–37. <https://doi.org/10.1016/j.cageo.2017.11.019>.